HYDROLOGICAL PROCESSES
Hydrol. Process. **28**, 1009–1024 (2014)
Published online 17 December 2012 in Wiley Online Library
(wileyonlinelibrary.com) DOI: 10.1002/hyp.9641

Spring drought prediction based on winter NAO and global SST in Portugal

João Filipe Santos,[1]* Maria Manuela Portela[2] and Inmaculada Pulido-Calvo[3]

[1] *Dpto. Engenharia, ESTIG, Instituto Politécnico de Beja, Rua Afonso III, Portugal*
[2] *Dpto. Engenharia Civil, SHRH, Instituto Superior Técnico (Lisboa), Portugal, Avda. Rovisco Pais, Lisboa, Portugal*
[3] *Dpto. Ciencias Agroforestales, Escuela Técnica Superior de Ingeniería, Campus La Rábida, Universidad de Huelva, Palos de la Frontera (Huelva), Spain*

Abstract:

The aim of this paper is to test the ability of neural network approaches to hindcast the spring standardized precipitation index on a 6-month time scale (SPI6) in Portugal, based on winter large-scale climatic indices. For this purpose, the linkage of the spring SPI time series with the winter North Atlantic Oscillation (NAO) and the sea surface temperature (SST) was investigated by means of maps of the correlation coefficient for the period from October 1910 to September 2004. The results indicate that the winter NAO is a good predictor for the SPI6 of the spring (SPI6 finishing in April, May and June, $SPI6_{April}$, $SPI6_{May}$ and $SPI6_{June}$, respectively) for the northern, central and southern regions of Portugal. The winter SST1 (area of the Mediterranean Sea) must only be considered for the northern region, and the winter SST3 (area of the North Atlantic between Iberia and North America) only for the southern region. Spatial maps of predictive SPI6 for April, May and June were created and validated. The neural models explained more than 81% of the total variance for the $SPI6_{April}$ and $SPI6_{May}$ and more than 64% of the total variance for the $SPI6_{June}$. Probability maps were also developed considering the values predicted by the neural methods for the spring months and all drought categories (moderate, severe and extreme). These maps indicating the probability of droughts can provide valuable support for the integrated planning and management of water resources throughout Portugal.

KEY WORDS artificial neural networks; hindcasting; standardized precipitation index; climatic indices; NAO

Received 10 July 2012; Accepted 25 October 2012

INTRODUCTION

In recent years, the seasonal forecast of hydroclimatological conditions has become an important scientific issue (Trigo *et al*., 2004; Rimbu *et al*., 2004, 2005; Gámiz-Fortis *et al*., 2008a,b; Ionita *et al*., 2008; Gámiz-Fortis *et al*., 2010). Compared with others of the most recurrent extreme events such as floods and hurricanes, drought is recognized as a phenomenon with adverse impacts that can potentially be effectively mitigated (Di Mauro *et al*., 2008). In fact, the consequences of drought take a long time to be perceived by socio-economic systems, in line with the fact that they tend to evolve slowly. An effective monitoring and forecasting system, able to promptly identify the onset of a drought and to follow its spatio-temporal evolution, represents one of the main prerequisites for implementing a successful mitigation strategy (Rossi, 2003).

Among the several climate variables that could be used to characterize droughts, precipitation is recognized as a key indicator of the occurrence and of the persistence of drought conditions (Lloyd-Hughes, 2002). According to Santos *et al*. (2005), precipitation is a primary variable in most hydrological models. Under the Mediterranean-type climatic conditions that prevail in Portugal, winter precipitation is one of the main factors in the water budgets of the hydrological cycle. Moreover, winter precipitation amounts play a key role in triggering drought episodes because, although natural and socio-economic systems are already prepared to cope with the Mediterranean summer dryness, they are not prepared for a lack of winter precipitation.

The North Atlantic Oscillation (NAO) has important connections with several climate variables and consequently with drought phenomena across Europe. This is clear from many studies including those of Hurrell and Van Loon (1997), Qian *et al*. (2000a,b), Hurrell *et al*. (2001), Trigo *et al*. (2002) and, more recently, López-Moreno *et al*. (2007) and Vicente-Serrano *et al*. (2011). Significant lag-correlation between drought patterns and the NAO suggests that it can be used as a potential predictor of European drought patterns on interannual time scales (Ionita *et al*., 2010).

Correlations between sea surface temperature (SST) and drought patterns across Europe have been recently explored in Ionita *et al*. (2010). On interannual time scales, these authors identified patterns of drought variability, which were strongly correlated with SST patterns from previous periods (years). According to the same authors, the time lag between drought and SST anomaly patterns can provide valuable information for the prediction of droughts over Europe on interannual time scales. For the USA, Wu and Kinter (2008) also show that drought could be linked to

*Correspondence to: João Filipe Santos, Dpto. Engenharia, ESTIG, Instituto Politécnico de Beja, Rua Afonso III, 7800-050, Portugal.
E-mail: joaof.santos@ipbeja.pt

anomalous SST. Hoerling and Kumar (2003) demonstrated the important contribution of persistent cold SST in the Tropical Eastern Pacific and warm SST in the Tropical Western Pacific-Indian Ocean to the 1998–2003 drought spanning from USA, to southern Europe and southwestern Asia. Schubert *et al.* (2004a,b) indicated the primary cause of the persistent drought in the USA in the 1930s was the anomalous tropical SST.

Climate conditions that vary on seasonal, interannual, and decadal time scales have a considerable influence in the availability of water and consequently on drought conditions. On seasonal time scales, Gámiz-Fortis *et al.* (2010) shown that anomalous atmospheric and oceanic conditions are often linked with seasonal variations in the precipitation and temperature (e.g. Dettinger and Díaz, 2000; Cullen *et al.*, 2002; Trigo *et al.*, 2004; Karabörk *et al.*, 2005; López-Moreno *et al.*, 2007; López-Moreno and Vicente-Serrano, 2008) and could, therefore, trigger drought phenomena and consequently variations in streamflow and reservoir storage. According to Gámiz-Fortis *et al.* (2010), the performance of the medium to long-range forecasts is associated with the introduction of predictors that represent the slow varying components of the climate system such as sea ice, snow cover, soil moisture, SSTs and major oceanic and atmospheric circulation patterns such as the El Niño–Southern Oscillation (ENSO), the NAO in Europe and the PNA in North America. Specifically, teleconnection patterns such as the NAO have a particularly strong impact on winter precipitation in the Iberian Peninsula which leads most of the studies of river flow prediction in that season (Trigo *et al.*, 2004; Gámiz-Fortis *et al.*, 2008a,b).

In the present study, the objective is to hindcast drought phenomena in Portuguese territory. Hindcasting is a way of testing or validating a model, by running it for a past time period and comparing results with observations. Due to the climate characteristics of Western Iberia, it is particularly important to ascertain whether hindcasting is sufficiently accurate when applied in early spring. In fact, the precipitation regime in the region is characterized by a primary peak in autumn and a secondary one in spring and by the absence of precipitation in summer (Martín *et al.*, 2004), which means once drought conditions develop in early spring they will continue at least until October (beginning of the rainy season and of the hydrological year). According to Lloyd-Hughes (2002), spring is found to be the most predictable season for European precipitation and consequently for drought. Results from an empirical model have shown that up to 35% of the variance in the springtime standardized precipitation index (SPI) over the region, can be predicted using a combination of data on the ENSO, local North Atlantic SST forcing and SPI from previous periods. Some other authors, such as García-Herrera *et al.* (2007), have also noted the importance of the lack of spring precipitation, in the understanding of the spatial extent of droughts and of their socio-economic impacts, as observed in the 2004/2005 drought. Furthermore, in contrast to the 2004/2005 event, in some other historical droughts studied by García-Herrera *et al.* (2007) there was recovery during spring months.

The index proposed herein for drought evaluation and hindcasting is the SPI (McKee *et al.*, 1993), which we have already used in other studies (Santos *et al.*, 2010, 2011, 2012) and has been widely applied in research in this field. Several authors have proposed methods to forecast or to assess the probable evolution of SPI (Cancelliere *et al.*, 2005; Bordi *et al.*, 2005; Moreira *et al.*, 2006; Cancelliere *et al.*, 2007a,b). Despite such efforts, to predict when a drought is likely to begin or to come to an end is still a difficult task (Cordery and McCall, 2000a,b). In this paper, our aim was to show that the consideration of external predictors in a hindcasting model, such as the NAO and SST, can potentially lead to improved prediction performance, as well as extending the time horizon of the prediction.

The analysis present used sequences of variables with values changing over time (multivariate time series). Various models have been proposed to deal with the random behaviour of such time series (Bras and Rodríguez-Iturbe, 1985). The most popular and widely used ones include simple and multiple linear regressions, autoregressive (AR), autoregressive moving average (ARMA) and autoregressive integrated moving average (ARIMA) models, and artificial neural network (ANN) models. As in Mishra and Desai (2006), Kim and Valdés (2003) and, more recently, Dastorani and Afkhami (2011), we used well-known ANN models for the hindcasting model for droughts.

The novelty of this work is that it explores the impact of large-scale predictors (SST) and major oceanic and atmospheric circulation patterns (NAO) on the spatial and temporal variability of drought-related fields in mainland Portugal, and it quantitatively assesses the capability of the models including these variables to hindcast droughts based on a new concept of probability maps for extreme drought events.

This paper is organized into four sections. With the background provided by this introductory section, we progress to the second section, which examines the materials and methodologies applied. After identifying the study area and the datasets used, the second section proceeds to a general description of the ANN models applied, with the analysis, based on maps of linear correlation, of the response of droughts to external (atmospheric and oceanographic) drivers and a description of the accuracy measures used for the model validation. It also addresses the uncertainty in the neural network predictions based on a new concept of probability maps for drought events. In the third section, the results are presented and discussed. Finally, conclusions are drawn and future research proposed in the fourth section.

MATERIALS AND METHODS

Study area and data synthesis

The research was focused on Portugal, a European country located in the western part of the Iberian Peninsula, spanning both Atlantic and Mediterranean climatic zones. The mean annual precipitation varies from more than 3000 mm, in the north-western region, to less than 400 mm, in the southern region, following a complex spatial pattern (N–S/E–W), closely connected with the topography, one of the most influential factors in the precipitation distribution. As the water availability decreases the hydrological regime (both over the year and between years) becomes more irregular (Portela and Quintela, 2006), and this makes the prediction of droughts an important issue for the water resources management, namely, in the semi-arid central and southern regions of the country.

In Santos *et al.* (2010), the general spatial pattern of droughts in Portugal was identified using the SPI computed on the basis of 94 years of monthly precipitation records (from October 1910 to September 2004) at 144 rain gauges located as illustrated in Figure 1. These authors demonstrated that Portugal can be considered in terms of three well-defined sub-regions or clusters with different patterns of drought, as represented in Figure 1: the north (cluster 1, CL1), the centre (cluster 2, CL2) and the south (cluster 3, CL3) of Portugal. There are 56, 53 and 35 rain gauges located in each of these sub-regions, respectively.

The present article contains the results from the application of ANN models with several predictors to hindcast droughts in the same three sub-regions for the spring months of April, May and June (AMJ). The ANN models were applied to each rain gauge in each region.

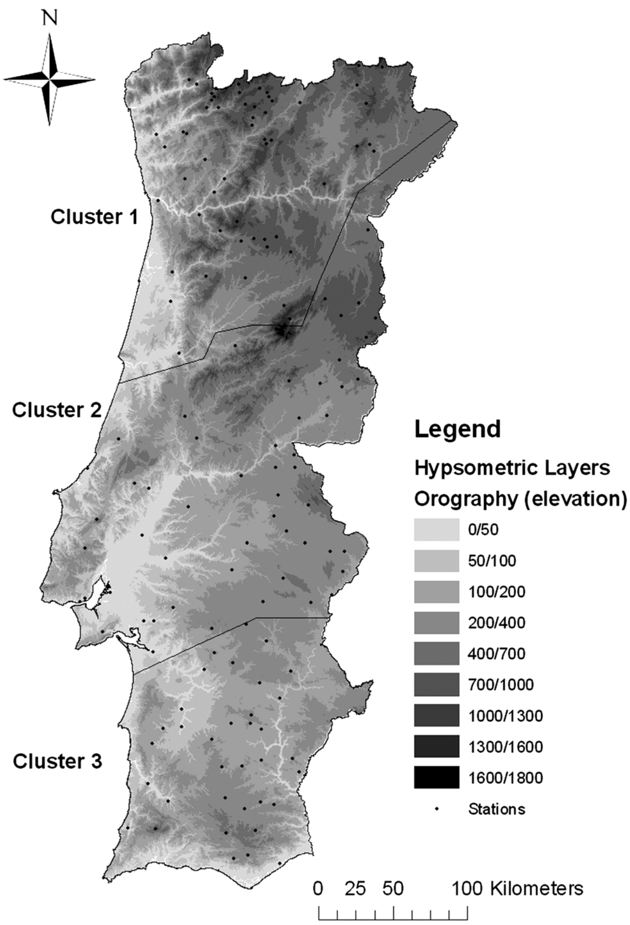

Figure 1. Spatial drought patterns in mainland Portugal using SPI. Map showing the three regions previously identified by cluster analysis (Santos *et al.*, 2010). The dots represent the location of the 144 rain gauges used for the drought analysis.

The drought information data to be hindcast was the 6-month SPI time series (SPI6), which quantifies the precipitation deficit on a 6-month time scale. Only the SPI indices for the spring months, which can really anticipate drought conditions under the climate conditions of mainland Portugal, are predicted: that is, SPI6 for the 6-month period finishing in April, May and June, $SPI6_{April}$, $SPI6_{May}$ and $SPI6_{June}$, respectively. WE chose to focus on SPI6 since the 6-month time scale provides a useful monitoring tool for agricultural drought assessment. According to Wilhite (2005), some water managers may prefer an indicator that responds quickly to short-term anomalies, such as the SPI3, to take early action to reduce drought impacts, whereas other water managers may prefer an indicator with greater stability and persistence, such as the SPI12, to avoid frequent invoking and revoking of drought-related measures. In the present study, the intermediate indicator was chosen, SPI6, with the aim of providing insights to both SPI3 and SPI12. Mo *et al.* (2009) stated that the SPI6 can be very effective in addressing the precipitation over distinct seasons and in identifying medium-term trends in precipitation and is still considered more sensitive to conditions at that scale than other indices (e.g. the Palmer Index).

Another issue is that in Portugal, some important economic activities are particularly prone to drought phenomena, such as non-irrigated agriculture (mainly cereals), where short SPI temporal scales such as the SPI6, indicative of agricultural drought, are more relevant. At the same time, an increase in tourism and irrigation have considerably raised the demand for water (in particular, in the southern drier regions), making water restrictions and economic losses of irrigated land due to hydrological droughts (established from a previous agricultural drought situation) more damaging to the economy and society (Vicente-Serrano, 2006; Pulido-Calvo *et al.*, 2012).

The predictors used were the global SST taken from the Extended Reconstructed SST v3b dataset developed by the National Oceanic and Atmospheric Administration's National Climatic Data Center (Smith *et al.*, 2007; Xue *et al.*, 2003) obtained from the Royal Netherlands Meteorological Institute (KNMI) Climate Explorer website. The spatial coverage used for SST fields was calculated based on two of the areas previously identified in the study of Gámiz-Fortis *et al.* (2010) and on the Mediterranean Sea. Specifically, the three main areas considered were: one covering the Mediterranean Sea – SST1 (37ºE-7ºW; 31ºN-47ºN); one close to Brazil, in the south-western Atlantic Ocean – SST2 (35ºW-25ºW; 15ºS-10ºS); and the North Atlantic between Iberia and North America – SST3 (45ºW-25ºW; 38ºN-42ºN). The SST monthly time series were obtained by averaging the cells within each of these regions (each cell with $2 \times 2°$ steps). Then, the winter SST fields were generated by normalizing the average monthly SST (January, February and March - JFM) by its mean and standard deviation for the period 1910/11-2003/04.

Gámiz-Fortis *et al.* (2008a,b) showed that a temporal autumn SST pattern, geographically representative of the same Atlantic region that was considered in the present study, is statistically significant correlated with the winter streamflow series at three key Portuguese watersheds. That study motivated us to consider the global STT as a predictor variable in the drought analysis.

Because the NAO is one of the main modes of atmospheric circulation that determines the climate of Europe (Hurrell *et al.*, 2003), we also decided to include this index as a predictor to assess whether its wintertime behaviour could be used to predict drought for the subsequent spring season. The NAO is recognized throughout the entire year in Europe, although it also shows important seasonal variability, which has led several authors to study the effect of NAO on droughts in the Iberian Peninsula including Zorita *et al.* (1992), Rodríguez-Puebla *et al.* (1998), Martín-Vide and Fernández (2001), Trigo and Palutikof (2001), Trigo *et al.* (2004) and Xoplaki *et al.* (2004). The NAO has a greater intensity and spatial coverage especially during winter (Hurrell *et al.*, 2003), with a known pattern of positive NAO phases being linked with dry conditions affecting southern Europe and increased precipitation affecting northern Europe (e.g. Hurrell and Van Loon, 1997; Trigo *et al.*, 2002; Hurrell *et al.*, 2003; and Silva *et al.*, 2012). The opposite pattern occurs during negative phases. Therefore, we used winter data (December, January and February), but we also included March in the winter NAO index to take into account early spring precipitation, which is very important in Portugal. The dataset selected here for the period from October 1910 to September 2004 was the NAO index as defined by Jones *et al.* (1997). For winter, the difference between the normalized sea level pressure over Gibraltar (in the southwest of the Iberian Peninsula) and that over Reykjavik (Iceland) is a useful indicator of the strength of the NAO (http://www.cru.uea.ac.uk/cru/data/vinther/nao1821.txt; Vinther *et al.*, 2003. In the present paper, the NAO index used was the one calculated based on the two aforementioned locations, instead of considering one of the dipoles as Lisbon or Ponta Delgada in the Azores. This choice was influenced by the fact that Jones *et al.* (1997) state that the choice of Gibraltar appears to better represent the southern part of the NAO dipole than other commonly used stations, such as Lisbon or Ponta Delgada. Furthermore, the conclusions of Hurrell (1995) and Jones *et al.* (2003) are extremely relevant for the purpose of this study, namely that the southwest European location used to calculate the NAO correlated slightly better with rain gauge precipitation series across Europe than information from the Azores used to calculate the NAO index.

Neural approaches – general procedure

Drought prediction plays an important role in the mitigation of several types of impact on water resources systems. Traditionally, statistical models have been used for hydrological drought forecasting based on time series methods. Models such as simple/multiple regression and ARMA techniques are typical statistical time series methods for forecasting. However, because they are basically linear models assuming that data are stationary and have a limited ability to capture non-stationarities and non-linearities in hydrological data, we have considered an alternative and more robust approach, namely an ANN model. As stated by the ASCE Task Committee on Application of Artificial Neural Networks in Hydrology (2000a,b) and confirmed by several authors (e.g. Dawson and Wilby, 1998; Ni *et al.*, 2002; Kim and Valdés, 2003; Mishra and Desai, 2006; Mishra *et al.*, 2007; Jain and Kumar, 2007; Pulido-Calvo *et al.*, 2012), ANNs have shown great ability in modelling and hindcasting non-linear and non-stationary time series in hydrology and water resources engineering because of their innate nonlinear property and flexibility for modelling.

The most widely studied and used ANN models involve multilayer feed-forward networks or multilayer perceptrons (MLP; Rumelhart *et al.*, 1986; Senthil-Kumar *et al.*, 2005). Some authors such as Mutlu *et al.* (2008) have also obtained better results with MLP than other types of ANN like radial basis functions (RBF).

In the present study, MLP models were used. These models 'learn' in an iterative way, the data provided being to the neural network multiple times until a pre-determined error level (calculated as the sum of the squared errors) is reached; each iteration is called an 'epoch'. These supervised ANNs allow the analysis of complex datasets and the assessment of non-linear relationships between dependent and independent variables. Detailed descriptions of multilayer perceptron ANNs have been given by Hsu *et al.* (1995), ASCE (2000a,b), Shrestha *et al.* (2005), Gutiérrez-Estrada *et al.* (2007), and Pulido-Calvo and Portela (2007). In particular, there are many methods for calibrating and training the ANNs; in this study, the standard back-propagation algorithm was used.

In this study, the ANN modelling scheme adopted was individual ANN calibration and validation for each of the rain gauge dataset, in each of the cluster regions (in total 144 ANN models for mainland Portugal) with drought information to be hindcasted (SPI6 for April, May and June). Prior to the calibration of any ANN, the SPI6 time series at each rain gauge was divided into two subsets: the test subset, TS, and the CSS subset, the latter comprising the calibration subset [CS] and the selected subset [SS]. The CSS subset included 75% of the data at each rain gauge of Figure 1 (68 years) and the TS subset the other 25% of the data (14 years). At each rain gauge we left the last 4 years of data (2001 to 2004) to run the validated individual ANN models in operational mode to produce and SPI6 spring maps for such years.

The best method to ensure that overtraining does not occur is to regularly monitor (at the end of each epoch) the sum of the square errors for both the CS and the SS subsets (internal validation). It is normal that the sum of the square errors for the CS subset decreases continuously with training. Eventually, however, this process may be forcing the neural network to fit the noise in the CS subset. To avoid this problem, training is paused at the end of each epoch and the sum of the square errors of the SS subset is calculated. When this sum begins to increase, training must be stopped and the weights of the epoch which provided the minimum error for the SS subset should be tested with the TS subset. This last step is also known as the generalization or external validation phase. Iyer and Rhinehart (1999) recommend repeating this process at least 30 times for each model. In this study, the process was repeated 100 times for each rain gauge to choose the best network.

The selection of the input variables from those available is a fundamental issue in ANN modelling (Bowden *et al.*, 2005; Shrestha *et al.*, 2005; May *et al.*, 2008; Fernando *et al.*, 2009). For calibration and validation phases, the objective is to select input variables that explain the highest percentage of the variance. Selection of inappropriate input variables may cause undesirable effects such as the naïve effect (i.e., outputs provided by the model for each period are systematically very close to values observed in the previous time periods), the presence of more local optima, and extreme difficulties in extracting physical meaning from the calibrated models. To overcome these problems, in the present study, linear relations between possible candidate inputs were previously assessed (via spatial linear correlation maps) and some of them were standardized before being incorporated into the MLP models.

The cumulative precipitation until March at each of the 144 rain gauges shown in Figure 1 was included as the main predictor of each spring SPI6. For that purpose, each cumulative precipitation series was normalized. For $SPI6_{April}$, $SPI6_{May}$ and $SPI6_{June}$, the period considered in the computation of the normalized cumulative precipitation was from November to March, December to March and January to March, respectively. The outputs of the models are the spring SPI6 values also for each of the rain gauges.

Within the external predictors considered, the SSTs were also normalized, as previously stated, and the NAO index is itself normalized, the data being normally distributed as in the case of the SPI.

Artificial neural networks with one and two hidden layers were then assessed; in each case, 5−50 neurons (5, 6, 7,. . ., 50) were tested. The sigmoid activation function was used in hidden neurons and the linear activation function was used in output neurons. To achieve one of the objectives of the study, we tested 100 ANN models for each rain gauge and for each SPI6 spring month to be predicted. For validation purposes, these models were then analysed based on error measures in order to identify the best model at each rain gauge and time series.

Neural networks can actually perform a number of regression and/or classification tasks simultaneously, although commonly each network performs only one. Accordingly, in most cases the network will have a single output variable, although in the case of many-state classification problems, this may correspond to a number of output units (the post-processing stage takes care of the mapping from output units to output variables). In the present study, we had intended to build a multivariate output network. However, the consideration of single networks with multiple output variables was found to lead to 'cross-talk' (i.e. hidden neurons experiencing difficulty learning, since they are attempting to model at least two functions at once), and the best results were obtained with the training of separate networks for each output ($SPI6_{April}$, $SPI6_{May}$ and $SPI6_{June}$) at each rain gauge. Problems with 'cross-talk' have been reported in other studies, including those of MacGregor and Gerstein (1991) and Craven *et al.* (1996).

Spatial linear correlation maps between spring SPI6 months and potential predictors

In seasonal hindcasting, the aim is to predict the spatial and temporal distribution of drought conditions a few months in advance. Even though the detailed dynamical evolution of atmospheric systems is not predictable for those time scales, some of their statistical features and main temporal patterns can be forecast.

To the best of our knowledge, no previous studies have addressed the impact of large-scale modes of atmospheric circulation and ocean conditions (e.g. NAO, ENSO, SOI, SST fields, etc.) on the spatial and temporal variability of drought-related fields in Portugal. Authors such as Sousa *et al.* (2011) have studied the potential links between some large-scale patterns and the inter-annual variability of self-calibrating Palmer Drought Severity Index (scPDSI) series and Trigo *et al.* (2006) carried out a comprehensive assessment of their impact on the Mediterranean precipitation and temperature fields. Specifically, the impact of the winter NAO on the occurrence of drought over Europe has been analysed in López-Moreno and Vicente-Serrano (2008), and Trigo *et al.* (2006) demonstrated that the magnitude of the average SPI anomalies is noticeably different for the positive and negative phases of the NAO, indicating an asymmetric response of droughts to the NAO.

To understand how the SSTs and one of the most important large-scale mode of atmospheric circulation (the NAO), here identified as external predictors, best describe the spring SPI6 fields, spatial linear correlation maps for mainland Portugal were obtained between each one of the spring SPI6 time series ($SPI6_{April}$, $SPI6_{May}$ and $SPI6_{June}$) and each one of the external predictors (SST1, SST2, SST3 and NAO). This analysis provided a basis on which to select input variables from among those available. This selection process is one of the major steps in

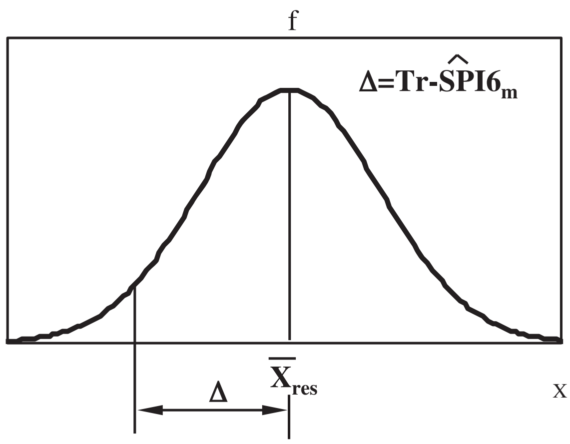

Figure 2. Probability of $\hat{SPI6}_m$ being less than a specific drought threshold (Tr) based on the normal distribution of the residuals

developing a satisfactory hindcasting model as the input variables determine the structure of the model and affect its results; it is also the first step before training and validating an ANN (Bowden *et al.*, 2005; Shrestha *et al.*, 2005; May *et al.*, 2008; Fernando *et al.*, 2009; Pulido-Calvo *et al.*, 2012).

Accuracy measures

To select the best ANN at each rain gauge and for each SPI6 to hindcast, four accuracy measures were used in the external validation: the square root of the mean square error (RMSE); the correlation coefficient (r); the efficiency coefficients (E_1 and E_2); and the persistence index (PI) (Nash and Sutcliffe, 1970; Kitanidis and Bras, 1980; Legates and McCabe, 1999; Pulido-Calvo and Portela, 2007). It is advisable to use the RMSE to quantify the error in the same units as the variables (in this case dimensionless SPI values). The square root of the mean square error (RMSE) is given by:

$$RMSE = \sqrt{\frac{\sum_{i=1}^{N}\left(SPI6_m - S\hat{P}I6_m\right)^2}{N}} \tag{1}$$

where $SPI6_m$ is the observed SPI6 time series at month m; $S\hat{P}I6_m$ is the hindcast SPI6 time series at month m; and N is the total number of observations of the validation set.

The coefficient of efficiency E_j is used to assess how well the hindcast values of SPI6 are similar to the observed SPI6 pattern. E_j is given by the following:

$$E_j = 1.0 - \frac{\sum_{i=1}^{N}\left|SPI6_m - S\hat{P}I6_m\right|^j}{\sum_{i=1}^{N}\left|SPI6_m - S\bar{P}I6\right|^j} \tag{2}$$

Table I. Drought categories according to the standardized precipitation index values (Agnew, 2000)

Non-exceedance probability	SPI	Drought category
0.05	>1.65	Extremely wet
0.10	>1.28	Severely wet
0.20	>0.84	Moderately wet
0.60	>-0.84 and <0.84	Normal
0.20	<-0.84	Moderate drought
0.10	<-1.28	Severe drought
0.05	<-1.65	Extreme drought

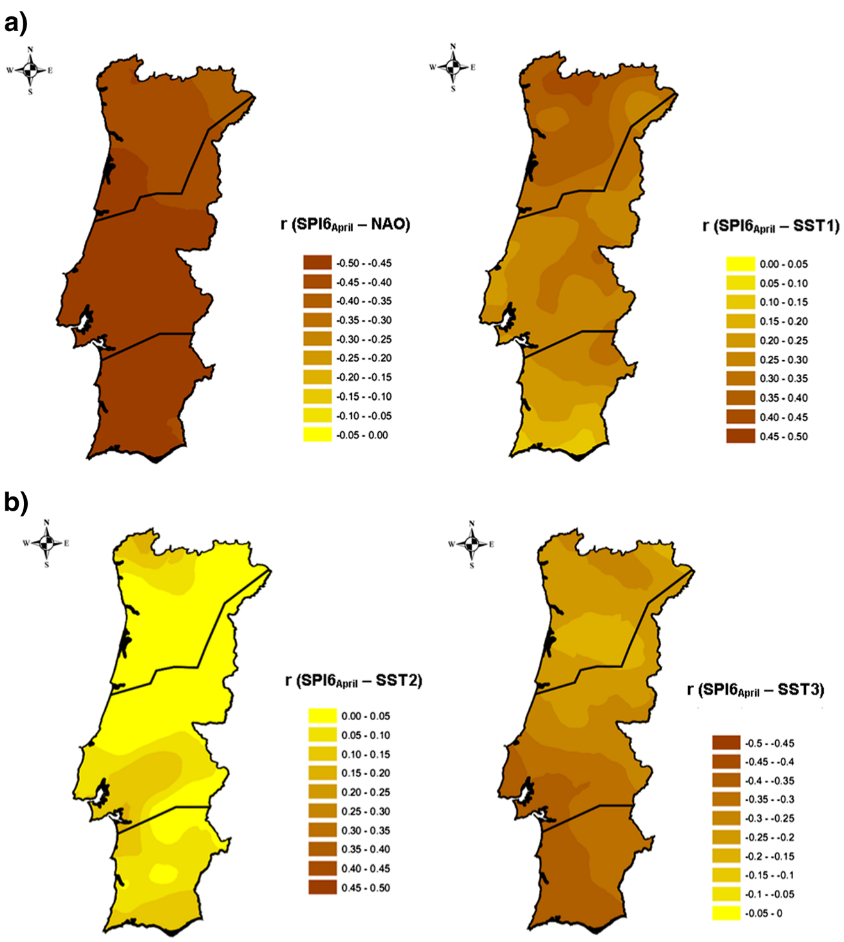

Figure 3. Maps of the linear correlation coefficient, r, between spring SPI6 months and each one of the external predictors: previous winter NAO and SST (SST1, SST2 and SST3). Period from October 1910 to September 2004

The sensitivity to outliers, due to the squaring of the difference terms, is reflected in E_2. The measure E_1 (here called the modified coefficient of efficiency) reduces the effect of the squared terms. A value of zero for E_2 indicates that the observed mean is as good predictor as the hindcast SPI6, whereas negative values indicate that the observed mean is a better predictor than the hindcast pattern (Legates and McCabe, 1999). For a good match, the values of R^2 and of E_j should be close to one.

Lastly, the PI used to evaluate the performance of the models is given by (Kitanidis and Bras, 1980):

$$PI = 1 \frac{\sum_{i=1}^{N} \left(SPI6_m - S\hat{P}I6_m\right)^2}{\sum_{i=1}^{N} \left(SPI6_m - SPI6_{m\text{-}L}\right)^2} \tag{3}$$

where $SPI6_{m\text{-}L}$ is the observed SPI value at the time step m-L and L is the lag time. In our calculations, L was set equal to one (only one year delay). A PI value of one reflects a perfect fit between observed and hindcast temporal patterns, and a value of zero is equivalent to saying that the model is no better than a 'naïve' model.

Uncertainty of neural models

To address the likelihood of the predictions given by each of the best ANNs models, for each of the rain gauges and spring SPI6 hindcast month, probability maps were generated based on the distribution of the residuals of the best ANN model. The residuals are defined as the SPI6 ANN hindcast estimates minus the SPI6 indices derived from the observations. At each rain gauge and for each time series, the residuals should be a random variable that is approximately normally distributed (i.e. the skewness coefficient is not significantly different from zero) with a null mean (Demyanov *et al*., 1998). To check the hypothesis of normality of the residuals, the test of Snedecor and Cochran (Snedecor and Cochran, 1989)

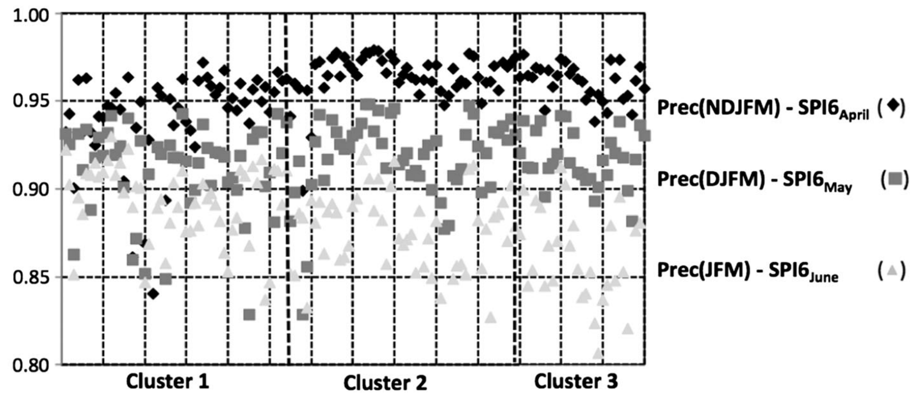

Figure 4. Correlation plot between spring SPI6 months and the normalized cumulative precipitation from November to March – Prec(NDJFM) – for SPI6April, from December to March – Prec(DJFM) – for SPI6May and from January to March – Prec(JFM) – for SPI6June. Dots are the different rain gauges in each cluster (total of 144 rain gauges).

Table II. Means of the accuracy measures for the best artificial neural networks in each region and for each spring SPI6 month

		$SPI6_{April}$				
		Mean accuracy measure				
ANN architecture	**Region**	***RMSE***	***r***	***E_1***	***E_2***	***PI***
3: 3 - (1 to 9) - 1: 1	**CL1**	0.292	0.960	0.749	0.915	0.961
2: 2 - (1 to 9) - 1: 1	**CL2**	0.210	0.977	0.811	0.953	0.975
3: 3 - (1 to 9) - 1: 1	**CL3**	0.250	0.975	0.786	0.946	0.972
		$SPI6_{May}$				
ANN architecture	**Region**	Mean accuracy measure				
		RMSE	***r***	***E1***	***E2***	***PI***
3: 3 - (1 to 9) - 1: 1	**CL1**	0.418	0.898	0.550	0.789	0.900
2: 2 - (1 to 9) - 1: 1	**CL2**	0.411	0.900	0.576	0.802	0.908
3: 3 - (1 to 9) - 1: 1	**CL3**	0.415	0.924	0.642	0.849	0.921
		$SPI6_{July}$				
ANN architecture	**Region**	Mean accuracy measure				
		RMSE	***r***	***E1***	***E2***	***PI***
3: 3 - (1 to 9) - 1: 1	**CL1**	0.460	0.828	0.434	0.667	0.828
2: 2 - (1 to 9) - 1: 1	**CL2**	0.517	0.780	0.367	0.596	0.791
3: 3 - (1 to 9) - 1: 1	**CL3**	0.548	0.796	0.393	0.623	0.772

was applied to each time series of residuals. According to that test, the hypothesis that the sample X is coming from a population with a normal distribution or, equivalently, the hypothesis that the skewness of X is not significantly different from zero, is rejected with the level of confidence η = 1-α, where α is the significance level, when:

$$\left|\frac{Ca_x}{(6/N)^{0.5}}\right| > \phi^{-1}(1-\alpha/2) \tag{4}$$

where Φ is the normal distribution function, Φ^{-1} the respective inverse normal distribution, N the sample size and Ca the sample skewness coefficient.

Table III. Time series of the residuals in each region. Average of the mean of the residuals and results from the Snedecor and Cochran test for each spring SPI6 month

	Region		
$\bar{X}_{res}$ **—residuals-**	**CL1**	**CL2**	**CL3**
$SPI6_{April}$	0.003	0.004	-0.001
$SPI6_{May}$	0.016	0.018	0.000
$SPI6_{June}$	0.019	0.000	-0.015
Snedecor and Cochran test (α = 5%) - residuals - [% non normal]	**Region (number of rain gauges)**		
	CL1 (56)	**CL2 (53)**	**CL3 (35)**
$SPI6_{April}$	14.29	7.55	2.86
$SPI6_{May}$	25.00	13.21	2.86
$SPI6_{June}$	17.86	7.55	20.00

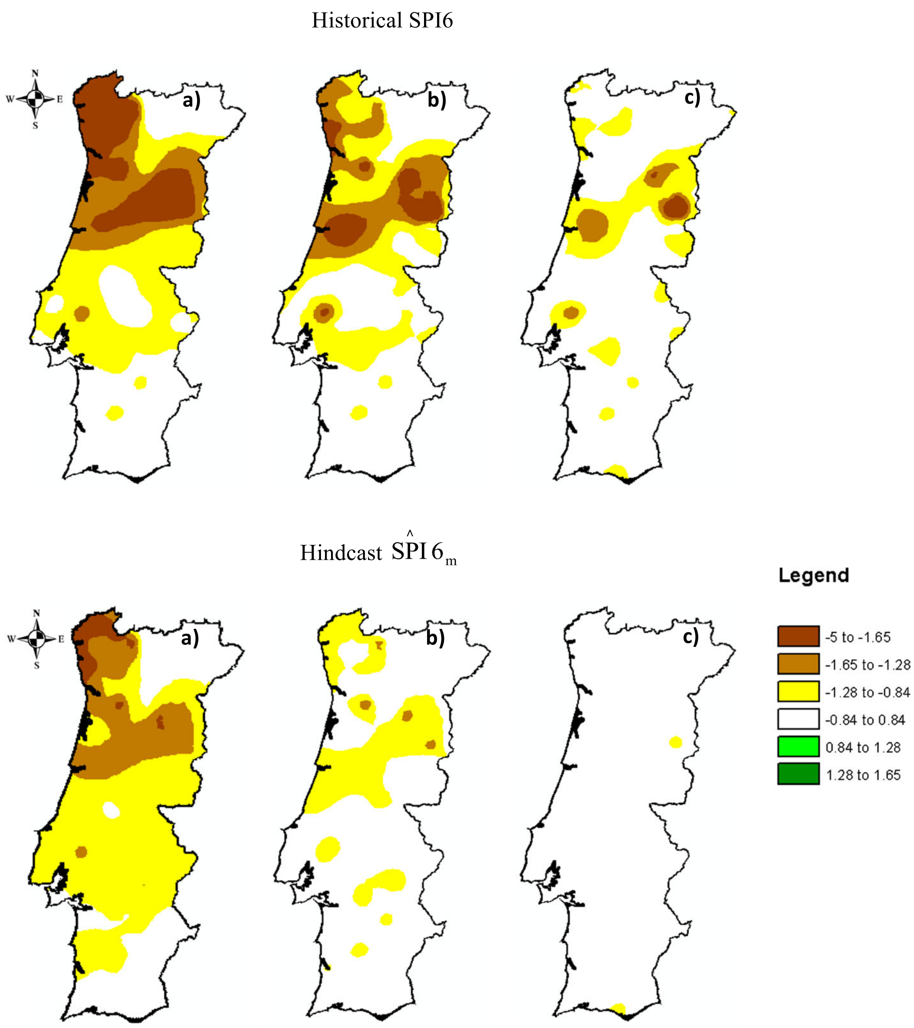

Figure 5. Historical and hindcast maps of SPI6 for the spring months: a) April, $SPI6_{April}$; b) May, $SPI6_{May}$; and c) June, $SPI6_{June}$ of 2002 (see Table I for the drought categories)

Probability maps for drought events

The generation of probability maps took into account the assumption of the normal distribution of the residuals at each rain gauge and for each spring SPI6 months. For each hindcast series, $S\hat{P}I6_m$, the probability of non-exceedance with respect to a specific drought category threshold, Tr, is given by Φ(Z), where Φ denotes the cumulative normal distribution function and Z the value of the standard normal variate given by (Figure 2):

$$Z = \frac{\left(Tr\text{-}S\hat{P}I6_m\right) - \bar{X}_{res}}{S_{res}} \quad (5)$$

where $\bar{X}_{res}$ and $S_{res.}$ are the mean and standard deviation of the residuals time series.

For each $S\hat{P}I6_m$ Φ(Z) gives the probability of having an $SPI6_m$ less than (or equal to) Tr, P ($SPI6_m \leq Tr$), according to the statistical characteristics of the residuals. The value of the drought threshold, Tr, was set on the basis of the drought categories proposed by Agnew (2000), presented in Table I.

RESULTS AND DISCUSSION

Selection of the input variables

The approach developed to hindcast the spring SPI6 months in Mainland Portugal used data on large-scale climatic fluctuations (NAO index) and sea surface temperatures (SST1 to SST3). To analyse the correlation between spring SPI6 time series ($SPI6_{April}$, $SPI6_{May}$ and $SPI6_{June}$) and both the large-scale climatic index and sea surface temperatures, spatial correlation maps, such as those exemplified in Figure 3, were obtained for the period from October 1910 to September 2004 considered in the analysis. Since the spatial correlation patterns are similar for the three SPI6 spring months, only the correlation maps for $SPI6_{April}$ are presented.

Figure 3 shows that the strength of the correlation was weak to moderate across most of the maps, with some values being statistically significant. According to Yevjevich (1972), for samples such as those analysed with 94 elements (years), linear correlations of 0.19 are significant at a confidence level of 5%.

The analysis indicates that NAO winter series are negatively correlated with spring SPI6 months, the best correlation values being obtained for central and southern regions (cluster 2 and 3). The ocean temperature anomaly

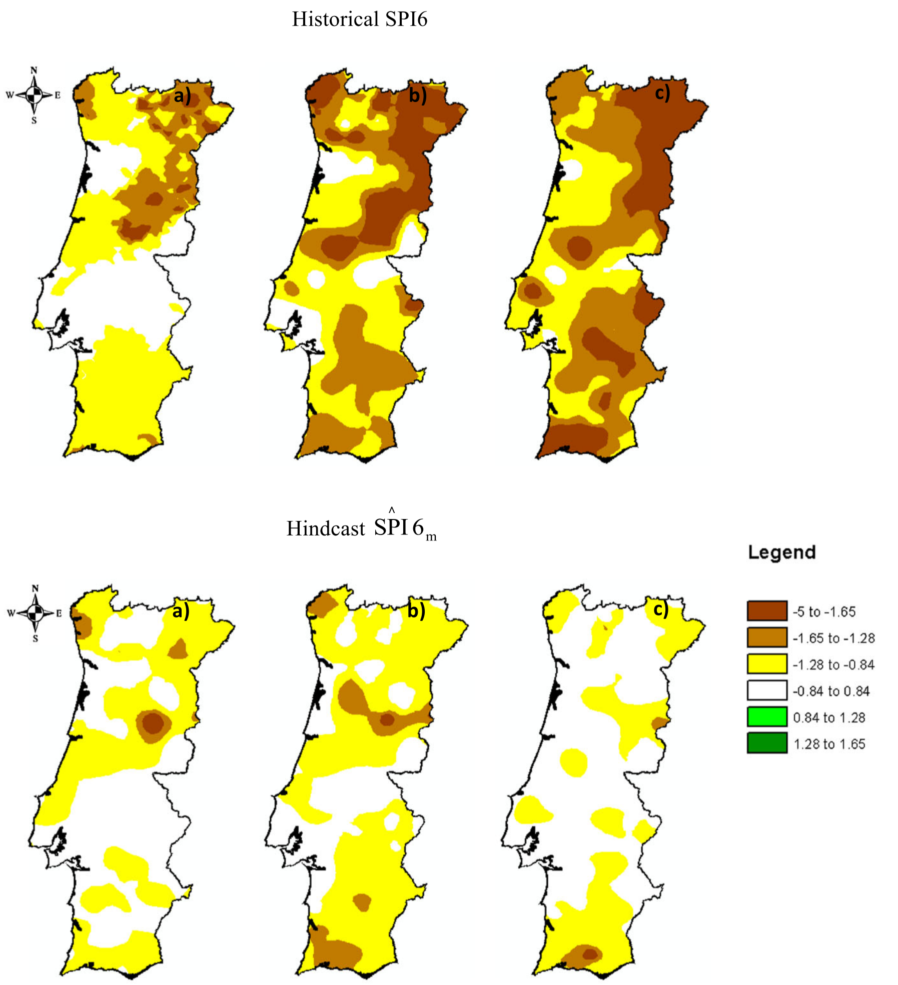

Figure 6. Historical and hindcast maps of SPI6 for the spring months: a) April, $SPI6_{April}$; b) May, $SPI6_{May}$; and c) June, $SPI6_{June}$ of 2004 (see Table I for the drought categories)

SST1 presents positive correlation in the northern region (cluster 1), the highest values being around 0.5. The correlations between SST2 and any of the SPI6 time series ($SPI6_{April}$, $SPI6_{May}$ and $SPI6_{June}$) were always very weak and not statistically significant. Accordingly, the external predictor SST2 was excluded from further analysis. For the SST3, significant negative correlations were obtained mainly in the coastal southern region, but with acceptable values for the entire southern region.

The results indicate that significant and stable indices such as the NAO, SST1 and SST3 can be potential external predictors for the hindcasting of SPI6 for April, May and June. In line with where the highest correlation coefficients were obtained, NAO was considered a potential predictor for the northern, central and southern region; while SST1 was only considered for the north and SST3 for the south. Based on these assumptions, multiple ANN multilayer perceptron hindcast models have been developed.

Since the precipitation is the most important trigger for drought monitoring and prediction, and is the only variable used to calculate SPI6, its reliability as a predictor was also assessed. The predictive variables related to the precipitation at each rain gauge were the normalized cumulative precipitation from November to March (NDJFM), from December to March (DJFM) and from January to March (JFM) for $SPI6_{April}$, $SPI6_{May}$ and

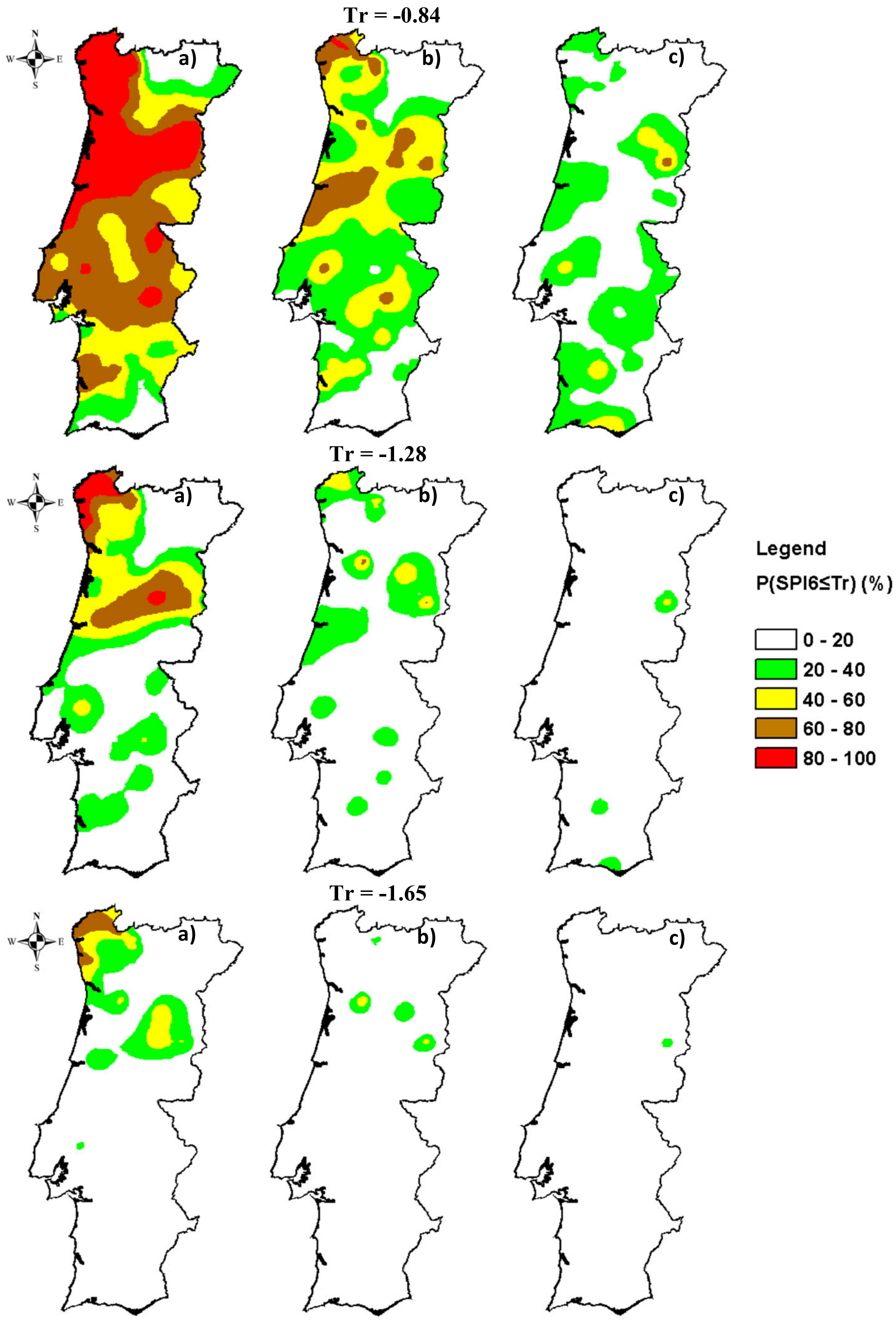

Figure 7. Probability maps for different drought thresholds, Tr, based on the predicted values of SPI6 for the spring months of: a) April, $SPI6_{April}$; b) May, $SPI6_{May}$; and c) June, $SPI6_{June}$ of 2002

$SPI6_{June}$, respectively. The precipitation months adopted as inputs for the hindcast spring SPI6 values are those considered in the SPI calculation, but until March, since the records in this last month of the winter period may play a significant anticipatory role in the hindcasting procedure.

The correlation coefficients between each one of the previous predictive variables and the respective SPI6 time series in the 144 rain gauges are plotted in Figure 4.

Figure 4 shows that stronger correlations are achieved for $SPI6_{April}$ with the respective standardized cumulative precipitation (NDJFM), followed by $SPI6_{May}$ (DJFM) and by $SPI6_{June}$ (JFM).

Validation of neural approaches: comparison of observed and hindcast maps (spatial and temporal distributions) of spring droughts

Table II reports the means of the accuracy measures of the best ANNs for the rain gauges included in each region of Figure 1. These results are quite good, especially for $SPI6_{April}$. In fact, for this spring drought index and for the central region (CL2), we found the lowest RMSE value (0.21), and the highest correlation r coefficient (0.98) while the measures E_1, E_2 and PI are the closest to one (0.81, 0.95 and 0.98, respectively).

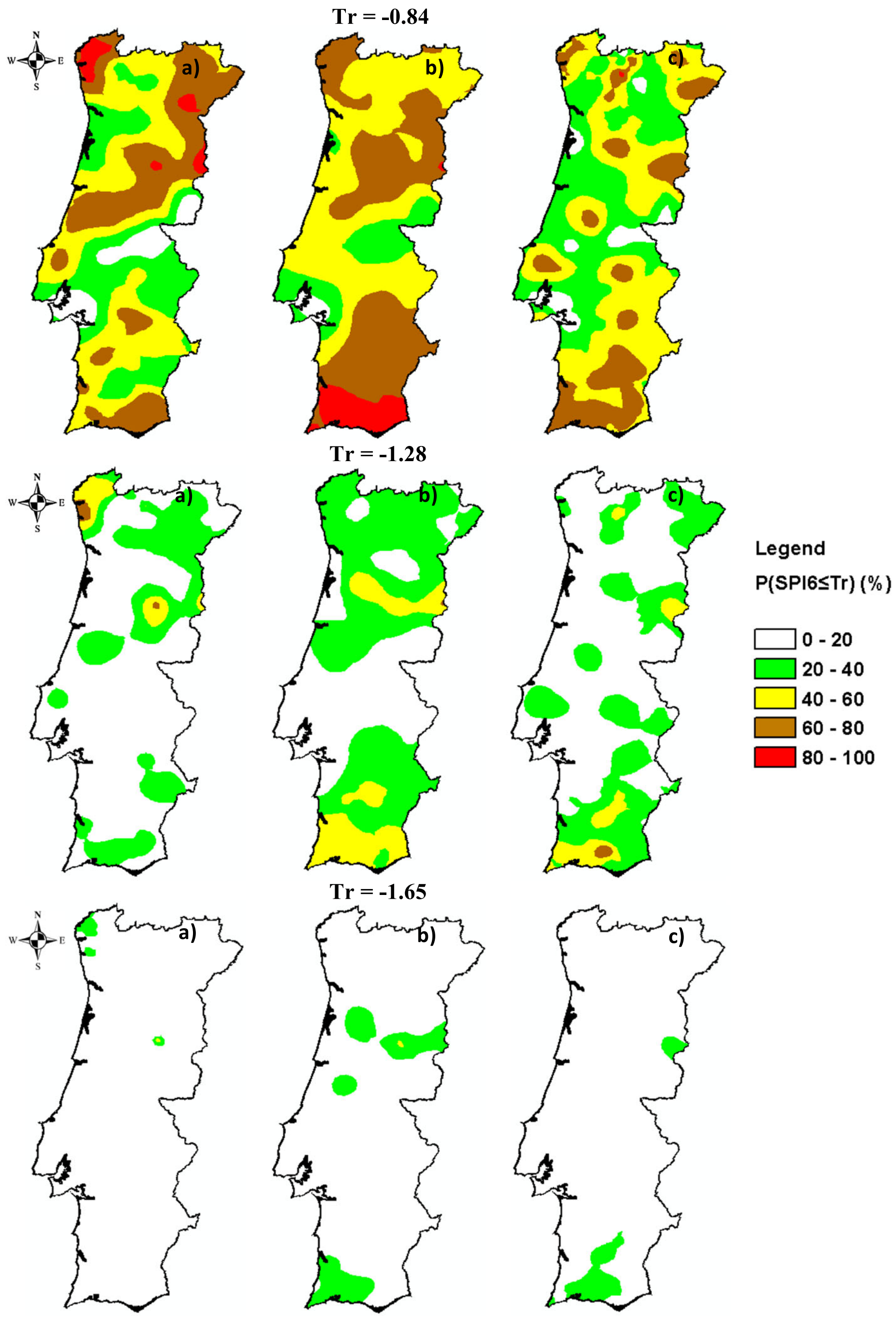

Figure 8. Probability maps for different drought thresholds, Tr, based on the predicted values of SPI6 for the spring months of: a) April, $SPI6_{May}$; b) May, $SPI6_{May}$; and c) June, $SPI6_{June}$ of 2004

In general terms, for a higher lag time in the hindcast the ANN fit the data progressively less well; this is noticeable when comparing the results of Table II sequentially for $SPI6_{April}$, $SPI6_{May}$ and $SPI6_{June}$. In fact, the means of the accuracy measures for $SPI6_{June}$ are worse than those for the other two spring months ($SPI6_{April}$ and $SPI6_{May}$). Nevertheless, the values obtained for $SPI6_{June}$ are still statistically reasonably good (RMSE < 0.55; r > 0.78; $E_1 > 0.37$; $E_2 > 0.60$; PI > 0.77).

According to Table III, the average of the mean of the residuals ($\bar{X}_{res}$) for the ANNs in each region is nearly 0, which is consistent with the normality assumption. Moreover, the distribution of the residuals was tested and found to be slightly skewed in only a few rain gauges; this fact also supports the assumption of symmetry and consequently of normality. The results of the Snedecor and Cochran test for normality at a significance level of 0.05 are also included in Table III. They show that cluster 1 (CL1) has the highest percentage of time series with non-normal residuals, with the hypothesis of normality rejected in one quarter of the rain gauges, for $SPI6_{May}$.

In this study, the drought hindcast multi-model approach was also addressed in a probabilistic sense with the goal of providing a quantitative assessment of the hindcast uncertainty and also because a 'reliable' probabilistic forecast enables more effective drought mitigation strategies to be adopted. Moye *et al.* (1988), for example, developed a probability distribution to predict the expected number of droughts with pre-specified duration, and the mean drought length over the desired time period based on the rudiments of run theory.

Figures 5 and 6 show the maps of the hindcast values of SPI6 for the spring months of 2002 and 2004 generated by the best ANN at each rain gauge. Those years were selected to exemplify the results achieved as they suffered the most severe drought events. Of the four years in the validation period, 2002 was a spring drought year that particularly affected the north coast, with clear recovery in terms of the drought areal extent and intensity between April and June. In 2004, a year with a generalized spring drought affecting the inland areas, the inverse occurred: the intensity and areal extent of the drought increased from April to June. Furthermore, in 2002, the areas most affected were the northern coast and an inland region near the border with Spain, while in 2004 the drought started in the north eastern part of Portugal and progressively expanded towards the west and south.

For April 2002, the estimates of the best ANN produce a pattern similar to the observed data. The performance is, however, significantly poorer in April 2004. It is relevant to note that, especially in the year 2004, the hindcast capabilities of the models are progressively less good for 2 and 3 months lag time (May and June, respectively). Figures 5 and 6 clearly indicate that the ANNs underestimate the extreme drought areas not being capable of reproducing the areal extent of the historical droughts.

Validation of neural approaches: probability maps of spatial and temporal distributions of spring droughts

Probability maps were also developed considering the values predicted by the neural approaches for the spring months of 2002 and 2004 (Figures 7 and 8). Each map represents the probability of having a drought of intensity equal to or more severe than a given threshold. The thresholds, Tr, considered were -0.84, -1.28 and -1.65 (drought categories of moderate, severe and extreme, respectively; Table I).

For the years of 2002 and 2004 and for the threshold of -0.84, the maps obtained based on the estimates of $SPI6_{April}$ indicate regions where the probability of having a drought with SPI less than or equal to -0.84 is very high and this is consistent with what really occurred (historical maps of Figures 5 and 6 based on the rainfall records). Despite the fact that this predictive capacity decreases as the lag time increases ($SPI6_{May}$ and $SPI6_{June}$) and especially for the spring of 2002, it still highlights the region that experienced drought. Further, as the threshold decreases towards more severe drought conditions, the probabilities of having droughts are less high. Nevertheless, they always identify the regions in which drought conditions did, in fact, develop.

Maps of the probability of drought events, such as those in Figures 7 and 8 can act as a fundamental support tool in drought forecasting and, consequently, in the integrated planning and management of water resources throughout a country or a region. The proposal of decision making under scenarios such as changes in the amount of water supplied, in water transfers between watersheds, in the reliability of the distributions systems, in hydropower production, and so on, could well benefit from the predictions obtained by this type of models several months in advance.

CONCLUSIONS

One of the most important steps in developing a satisfactory hindcasting model is the selection of the input variables. These variables determine the structure of the hindcasting model and affect its results. In the present study, the hindcasting structure developed for spring SPI6 months in mainland Portugal was based on neural approaches (ANN modelling) and incorporated information on large-scale climatic fluctuations (NAO index) and sea surface temperatures (SST1 and SST3). The presence of an influence of winter the NAO on spring SPI6 months was assessed with correlation analysis, for each of the main drought areas previously identified for mainland Portugal (north, centre and south), and we observed significant correlations at a 95% confidence interval. The NAO has been widely used to predict drought conditions with a high degree of reliability (e.g. Cordery and McCall, 2000a,b; Rodwell, 2003), although, López-Moreno and Vicente-Serrano, 2008, demonstrated considerable instability in the influence of positive and negative phases of the NAO on Europe-wide droughts that still needs to be further investigated.

According to the latter authors, this instability complicates the prediction and management of droughts based solely on the wintertime NAO index. This comment is consistent with our results since our effective modelling is not based uniquely on the NAO and, at the same time, backs the synergetic approach adopted here, with two external variables being added to the hindcast process.

The sea surface temperatures (SST1 and SST3) from some of the selected locations were also found to have different but significant correlations with spring SPI6 months regarding the drought area and the month to predict. This analysis of possible relations between different SSTs locations and spring SPI6 months, conducted in the first part of the paper, had the objective of testing this new forecasting tool, since SST patterns can induce different rainfall patterns and hence different drought patterns. Several forecasting models have been explored considering the associations between precipitation and lagged SST for different regions of the Atlantic area of Europe including those of Philips and McGregor (2002); Philips and Thorpe (2006); and Lorenzo *et al*. (2010). The latter authors demonstrated that the Pacific Ocean SST could be a suitable variable to forecast spring rainfall anomalies in NW Iberian Peninsula for the period 1951–2006.

Several other regions of the world have been analysed based on methodologies similar to the one considered here for hindcasting drought. In Iran, Jamshidi *et al*. (2011) applied MLPs to forecast values of SPI at five synoptic stations. MLPs were built to permit one month lead time forecasting using four different input vectors. Models were constructed by importing antecedent SPI values with one, two, three and four month time lags and antecedent precipitation with one and two month time lags. Additionally, antecedent NAO and Southern Oscillation Index (SOI) values with one month time lag were also considered. For Sicily (Italy), Cutore *et al*. (2009) used ANNs to forecast drought situations based on the Palmer Drought Index and have extended the models in order to include other indices, such as NAO and European Blocking (EB). For Iran, Jamshidi *et al*. (2011) noticed that the addition of NAO and SOI values as input variables to the MLPs, improved the prediction efficiency of their models, while for Sicily the results of Cutore *et al*. (2009) also indicate good improvements in terms of the correlation in the forecasting model between the prediction for winter and autumn months obtained when the NAO index and, especially, the EB index were considered. In the latter region and contrary to our results, the model behaved differently for the spring and summer predictions since they noticed no significant improvements in terms of model predictive capability with the introduction of the climatic indices as input variables. In this case, we believe that the poor performance of those models for the spring and summer months are mainly explained by the less significant influence of the winter NAO on Sicily, recognized by the weakness of the correlation between the NAO and the PDSI for the aforementioned season (Cutore *et al*., 2009). Others authors have also noticed some instability in the influence of the NAO signal when they tried to estimate drought class transition probabilities in southern Italy (Di Mauro *et al*., 2008). This was not a problem for our region since the Iberian Peninsula (Portugal and Spain) is one of the European areas recognized to the most strongly affected by the NAO (López-Moreno and Vicente-Serrano, 2008).

The results we achieved were based on time lags between the predictors and the hindcast variable that were different to the lags used in all the previous studies cited. In our opinion, this underlines the need to investigate the effect of the lag-time between the winter NAO and SST in different locations with the spring SPI at several time scales. Some clues can be used as a starting point, such as the results of a study for southern Europe by Trigo *et al*. (2004), which documented a lag time of 2–3 months in the response of river discharge to NAO positive and negative phases in the Atlantic basins of the Iberian Peninsula. The literature indicates features common to all forecasting models, namely the fact that the prediction efficiency for higher SPI time scales is increasingly better than for the lower SPI time scales and that the consideration of different hydrological zones does not influence final results. These aspects need to be clarified in our case.

Furthermore, the methodology applied in this study followed some of the recommendations of Kurnik (2009): that drought forecasting should be done with probabilistic approach and that an integrated drought forecasting methodology is also necessary, using both hydrological indicators (e.g. soil moisture, low flows, etc.) and meteorological indicators (e.g. SPI, PDSI, etc.). This latter recommendation needs to be addressed in further research.

Water managers and agricultural activities could strongly benefit from a forecasting system that could provide a probabilistic estimate a few months in advance, spring being the most sensitive season for drought analysis. Long historical SPI time series are essential components of a reliable forecasting model, as they are what make it possible to achieve good fits with ANN models.

The disadvantage of using statistical models to forecast is the possible non-stationary nature of the historical correlations among global variables (e.g. SSTs and NAO) and regional climate (e.g. SPI6) due to climate change. Regarding the present study, further research should be conducted to improve our understanding of such historical relations and patterns. From the historical record, we know that climate is inherently variable. We also know that anomalies of precipitation and temperature may last from several months to several decades. How long they last depends on air–sea interactions, soil moisture and land surface processes, topography, internal dynamics, and the accumulated influence of dynamically unstable synoptic weather systems at the global scale. On the other hand, the potential for improved drought predictions in the near future differs by region, season, and climatic regime.

The less good performance of the multiple models of ANNs, especially in the spring of 2004, could be related to the fact that this was an extreme drought year. It is recognized that the ANNs are not very good at reproducing extreme values even if they were present to some extent in the historical time series with which the ANN model was calibrated. Notably, Dawdson and Wilby (1998) and Campolo *et al*. (1999) suggested that underestimation in neural network models could be attributed to a lack of information provided to the network. Others, such as Karunanithi *et al*. (1994), suggested promisingly that including more extreme values patterns in the training data sets could alleviate the problem. Regarding our work, these aspects need further research.

REFERENCES

Agnew CT. 2000. Using the SPI to identify drought. *Drought Network News* **12**: 6–12.

ASCE Task Committee on Application of Artificial Neural Networks in Hydrology. 2000a. Artificial neural networks in hydrology. I. Preliminary concepts. *Journal of Hydrology Engineering* **5**(2): 115–123.

ASCE Task Committee on Application of Artificial Neural Networks in Hydrology. 2000b. Artificial neural networks in hydrology. II. Hydrologic applications. *Journal of Hydrology Engineering* **5**(2): 124–137.

Bordi I, Fraedrich K, Petitta M, Sutera A. 2005. Methods for predicting drought occurrences. In *Proceedings of the 6th International Conference of the European Water Resources Association*, Menton, France.

Bowden GJ, Dandy GC, Maier HR. 2005. Input determination for neural network models in water resources applications. Part 1—background and methodology. *Journal of Hydrology* **301**: 75–92.

Bras RL, Rodríguez-Iturbe I. 1985. *Random functions and hydrology*. Addison-Wesley: Massachusetts, USA.

Campolo M, Andreusi P, Soldati A. 1999. River flood forecasting with a neural network model. *Water Resources Research* **35**(10): 1191–1197.

Cancelliere A, Di Mauro G, Bonaccorso B, Rossi G. 2005. Stochastic forecasting of Standardized Precipitation Index. In *Proceedings of XXXI IAHR Congress Water Engineering for the future: Choice and Challenges*, Seoul, Korea, 3252-3260.

Cancelliere A, Di Mauro G, Bonaccorso B, Rossi G. 2007a. Drought forecasting using the Standardized Precipitation Index. *Water Resources Management* **21**(5): 801–819.

Cancelliere A, Di Mauro G, Bonaccorso B, Rossi G. 2007b. Investigating the potential of NAO index to forecast droughts in Sicily. Conference AGU, Hydrology Days, Colorado University, USA.

Cordery I, McCall M. 2000a. A model for forecasting drought from teleconnections. *Water Resources Research* **36**: 763–768.

Cordery I, McCall M. 2000b. A model for forecasting drought from teleconnections. *Water Resources Research* **36**: 763–768.

Craven MP, Curtis KM, Hayes-Gill BR. 1996. Multiple channel crosstalk removal using limited connectivity neural networks. Proceedings of the third IEEE International Conference on Electronics, Circuits and Systems, Rhodes, Greece, vol. 2, 1104–1107.

Cullen HM, Kaplan A, Arkin PA, Demenocal PB. 2002. Impact of the North Atlantic Oscillation on Middle Eastern climate and streamflow. *Climatic Change* **55**: 315–338.

Cutore P, Di Mauro G, Cancelliere A. 2009. Forecasting Palmer Index Using Neural Networks and Climatic Indexes. This paper is part of the *Journal of Hydrologic Engineering* **14**(6): June 1. ISSN 1084-0699/2009/6-588-595.

Dastorani MT, Afkhami H. 2011. Application of artificial neural networks on drought prediction in Yazd (Central Iran). *DESERT* **16**: 39–48.

Dawdson CD, Wilby R. 1998. An artificial neural network approach to rainfall-runoff modeling. *Journal of Hydrological Sciences* **43**: 14–66.

Dawson DW, Wilby R. 1998. An artificial neural network approach to precipitation-runoff modeling. *Hydrological Sciences Journal* **43**(1): 47–65.

Demyanov V, Kanevsky M, Chernov S, Savelieva E, Timonin V. 1998. Neural network residual kriging application for climatic data. *Journal of Geographic Information and Decision Analysis* **2**(2): 215–232.

Dettinger MD, Díaz HF. 2000. Global characteristics of streamflow seasonality and variability. *Journal of Hydrometeorology* **1**: 289–310.

Di Mauro G, Bonaccorso GB, Cancelliere A, Rossi G. 2008. Use of NAO index to improve drought forecasting in the Mediterranean area: Application to Sicily region. Options Méditerranéennes. Série A: Séminaires Méditerranéens, No. 80.

Fernando MKG, Maier HR, Dandy GC. 2009. Selection of input variables for data driven models: An average shifted histogram partial mutual information estimator approach. *Journal of Hydrology* **367**: 165–176.

Gámiz-Fortis S, Pozo-Vázquez D, Trigo RM, Castro-Díez Y. 2008a. Quantifying the predictability of winter river flow in Iberia. Part I: Interannual predictability. *Journal of Climate* **21**: 2484–2502.

Gámiz-Fortis S, Pozo-Vázquez D, Trigo RM, Castro-Díez Y. 2008b. Quantifying the predictability of winter river flow in Iberia. Part II: Seasonal predictability. *Journal of Climate* **21**: 2503–2518.

Gámiz-Fortis S, Esteban-Parra MJ, Trigo RM, Castro-Díez Y. 2010. Potential predictability of Iberian river flow based on its relationship with previous winter global SST. *Journal of Hydrology* **385**: 143–149.

García-Herrera R, Paredes D, Trigo RM, Trigo IF, Hernández E, Barriopedro D, Mendes MA. 2007. The outstanding 2004/05 drought in the Iberian Peninsula: Associated atmospheric circulation. *Journal of Hydrometeorology* **8**: 483–498.

Gutiérrez-Estrada JC, Silva C, Yáñez E, Rodríguez N, Pulido-Calvo I. 2007. Monthly catch forecasting of anchovy *Engraulis ringens* in the north area of Chile: Non-linear univariate approach. *Fisheries Research* **86**: 188–200.

Hoerling M, Kumar A. 2003. The perfect ocean for drought. *Science* **299**: 691–694.

Hsu K, Gupta HV, Sorooshian S. 1995. Artificial neural network modeling of the precipitation-runoff process. *Water Resources Research* **31**(10): 2517–2530.

Hurrell JW. 1995. Decadal trends in North Atlantic Oscillation: Regional temperatures and precipitation. *Science* **269**: 676–679.

Hurrell JW, Van Loon H. 1997. Decadal variations in climate associated with the North Atlantic Oscillation. *Climate Change* **36**: 301–326.

Hurrell JW, Kushnir Y, Visbeck M. 2001. The North Atlantic Oscillation. *Science* **291**: 603–605.

Hurrell JW, Kushnir Y, Ottersen G, Visbeck M. 2003. The North Atlantic Oscillation: Climatic significance and environmental impact. Geophysical Monograph Series, 134, American Geophysical Union, Washington, DC, USA.

Ionita M, Lhomann G, Rimbu N. 2008. Prediction of spring Elbe discharge based on stable teleconnections with winter global temperature and precipitation. *Journal of Climate* **21**(23): 6215–6226.

Ionita M, Lohmann G, Rimbu N, Chelcea S. 2010. Interannual to decadal summer drought variability over Europe and its relationship with global sea surface temperature. Geophysical Research Abstracts 12, EGU2010-8454, EGU General Assembly 2010, Viena, Austria.

Iyer MS, Rhinehart RR. 1999. A method to determine the required number of neural-network training repetitions. *IEEE Transactions on Neural Networks* **10**(2): 427–432.

Jain A, Kumar AM. 2007. Hybrid neural network models for hydrologic time series forecasting. *Applied Soft Computing* **7**(2): 585–592.

Jamshidi H, Arian A, Rezaeian-Zadeh M. 2011. Drought forecasting by Multilayer Perceptron network in Different climatological regions. ICID 21st International Congress on Irrigation and Drainage, 15-23, Thehran, Iran.

Jones PD, Jónsson T, Wheeler D. 1997. Extension to the North Atlantic Oscillation using early instrumental pressure observations from Gibraltar and South-West Iceland. *International Journal of Climatology* **17**: 1433–1450.

Jones PD, Osborn TJ, Briffa KR. 2003. Pressure-based measures of the North Atlantic oscillation (NAO): A comparison and an assessment of changes in the strength of the NAO and in its influence on surface climate parameters. The North Atlantic Oscillation: Climate Significance and Environmental Impact. Geophysics Monogram, Vol. 134, American Geophysical Union, 51–62.

Karabörk MÇ, Kahya E, Karaca M. 2005. The influences of the Southern and North Atlantic Oscillations on climatic variables in Turkey. *Hydrological Processes* **19**: 1185–1211.

Karunanithi N, Grenney WJ, Whitely D, Bovee K. 1994. Neural networks for river flow prediction. *Journal of Computing in Civil Engineering* **8**: 201–219.

Kim T, Valdés JB. 2003. Nonlinear Model for Drought Forecasting Based on a Conjunction of Wavelet Transforms and Neural Networks. *Journal of Hydrologic Engineering* **8**(6): 319–328.

Kitanidis PK, Bras RL. 1980. Real time forecasting with a conceptual hydrological model. 2. Applications and results. *Water Resources Research* **16**(6): 1034–1044.

Kurnik B. 2009. DESERT Action JRC, Drought forecasting methods. Ljubljana on 24 September 2009 – 1st DMCSEE – JRC Workshop on Drought Monitoring.

Legates DR, McCabe Jr. GJ. 1999. Evaluating the use of 'goodness-of-fit' measures in hydrologic and hydroclimatic model validation. *Water Resources Research* **35**(1): 233–241.

Lloyd-Hughes B. 2002. The long range predictability of European drought. PhD Thesis, Department of Space and Climate Physics, University of London, University College London, UK.

López-Moreno JI, Vicente-Serrano SM. 2008. Extreme phases of the wintertime North Atlantic Oscillation and drought occurrence over Europe: a multi-temporal-scale approach. *Journal of Climate* **21**: 1220–1243.

López-Moreno JI, Beguería S, Vicente-Serrano SM, García-Ruiz JM. 2007. The influence of the NAO on water resources in central Iberia: Precipitation, streamflow anomalies and reservoir management strategies. *Water Resources Research* **43**: W09411. DOI: 10.1029/2007WR005864.

Lorenzo MN, Taboada JJ, Iglesias I. 2010. Predictability of the spring rainfall in Northwestern Iberian Peninsula from sea surfaces temperature of ENSO areas. *Journal of Climatic Change*. DOI: 10.1007/s10584-010-9991-6.

MacGregor RJ, Gerstein GL. 1991. Cross-talk theory of memory capacity in neural networks. *Biological Cybernetics* **65**(5): 351–355.

Martín ML, Luna MY, Morata A, F Valero. 2004. North Atlantic teleconnection patterns of low-frequency variability and their links with springtime precipitation in the western Mediterranean. *International Journal of Climatology* **24**: 213–230.

Martín-Vide J, Fernández D. 2001. El índice NAO y la precipitación mensual en la España peninsular. *Investigaciones Geográficas* **26**: 41–58.

May RJ, Maier HR, Dandy GC, Fernando TMKG. 2008. Non-linear variable selection for artificial neural networks using partial mutual information. *Environmental Modelling and Software* **23**(10–11): 1312–1326.

McKee TB, Doesken NJ, Kleist J. 1993. The relationship of drought frequency and duration to time scales. In *Proceedings of the 8th Conference on Applied Climatology*. American Meteorological Society, Boston, USA, 179–184.

Mishra AK, Desai VR. 2006. Drought forecasting using feed-forward recursive neural network. *Ecological Modelling* **198**(1-2): 127–138.

Mishra AK, Desai VR, Singh VP. 2007. Drought forecasting using a hybrid stochastic and neural network model. *Journal of Hydrologic Engineering* **12**(6): 626–638.

Mo KC, Jae-Kyung E, Schemm E, Yoo S-H. 2009. Influence of ENSO and the Atlantic multi-decadal Oscillation on drought over the United States. *Journal of Climate* **22**: 5962–5982.

Moreira EE, Paulo AA, Pereira LS, Mexia JT. 2006. Analysis of SPI drought class transitions using loglinear models. *Journal of Hydrology* **331**(1-2): 349–359.

Moyé LA, Kapadia AS, Cech IM, Hardy RJ. 1988. The theory of runs with applications to drought prediction. *Journal of Hydrology* **103**(1-2): 127–137.

Mutlu E, Chaubey I, Hexmoor H, Bajwa SG. 2008. Comparison of artificial neural network models for hydrologic predictions at multiple gauging stations in an agricultural watershed. *Hydrological Processes* **22**(26): 5097–5106.

Nash JE, Sutcliffe JV. 1970. River flow forecasting through conceptual models. I. A discussion of principles. *Journal of Hydrology* **10**: 282–290.

Ni F, Cavazos T, Hughes MK, Comrie AC, Funkhouser G. 2002. Cool-season precipitation in the southwestern USA since AD 1000: Comparison of linear and nonlinear techniques for reconstruction. *International Journal of Climatology* **22**: 1645-1662.

Philips ID, McGregor GR. 2002. The relationship between monthly and seasonal south-west England rainfall anomalies and concurrent North Atlantic sea surface temperatures. *International Journal of Climatology* **22**: 197–217.

Philips ID, Thorpe J. 2006. Icelandic precipitation-North Atlantic sea-surface temperature associa- tions. *International Journal of Climatology* **26**: 1201–1221.

Portela MM, Quintela AC. 2006. Estimação em Portugal Continental de escoamento e de capacidades úteis de albufeiras de regularização na ausência de informação. *Recursos Hidrícos* **27**(2): 7–18.

Pulido-Calvo I, Portela MM. 2007. Application of neural approaches to one-step daily flow forecasting in Portuguese watersheds. *Journal of Hydrology* **332**: 1–15.

Pulido-Calvo I, Gutiérrez-Estrada JC, Savic D. 2012. Heuristic modelling of the water resources management in the Guadalquivir River Basin, Southern Spain. *Water Resources Management* **26**: 185–209.

Qian BJ, Xu H, Corte-Real JM. 2000a. Is the North Atlantic Oscillation the most important atmospheric pattern for precipitation in Europe? *Journal of Geophysical Research* **105**: 901–910.

Qian BJ, Xu H, Corte-Real JM. 2000b. Spatial–temporal structures of the quasi-periodic oscillations in precipitation over Europe. *International Journal of Climatology* **20**: 1583–1598.

Rimbu N, Dima M, Lohmann G, Stefan S. 2004. Impacts on the North Atlantic Oscillation and the El Niño-southern oscillation on Danube River flow variability. *Geophysical Research Letters* **31**: L23203. DOI: 10.1029/2004GL020559.

Rimbu N, Dima M, Lohmann G, Musat I. 2005. Seasonal prediction of Danube flow variability based on stable teleconnection with sea surface temperature. *Geophysical Research Letters* **32**: L21704. DOI: 10.1029/2005GL0224241.

Rodríguez-Puebla C, Encinas AH, Nieto S, Garmendia J. 1998. Spatial and temporal patterns of annual precipitation variability over the Iberian Peninsula. *International Journal of Climatology* **18**: 299–316.

Rodwell MJ. 2003. On the predictability of North Atlantic Climate, in the North Atlantic Oscillation: climatic significance and environmental impact. *Geophysical Monography Series* **134**: 173–192. DOI:10.1029/134GM08.

Rossi G 2003. Requisites for a drought watch system. In *Tools for Drought Mitigation in Mediterranean Regions*, Rossi G, *et al*. (eds). Kluwer Academic Publishing: Dordrecht; 147–157.

Rumelhart DE, Hinton GE, Williams RJ. 1986. 'Learning' representations by backpropagation errors. *Nature* **323**: 533–536.

Santos JA, Corte-Real J, Leite SM. 2005. Weather regimes and their connection to the winter precipitation in Portugal. *International Journal of Climatology* **25**: 33–50.

Santos JF, Pulido-Calvo I, Portela MM. 2010. Spatial and temporal variability of droughts in Portugal. *Water Resources Research* **46L**: W03503. DOI: 10.1029/2009WR008071.

Santos JF, Portela MM, Pulido-Calvo I. 2011. Regional frequency analysis of droughts in Portugal. *Water Resources Management* **25**(14): 3537–3558.

Santos JF, Portela MM, Pulido-Calvo I. 2012. Dimensionality reduction in drought modelling. *Hydrological Processes*. DOI: 10.1002/hyp.9300 (published on-line).

Schubert SD, Suarez MJ, Pegion PJ, Koster RD, Bacmeister JT. 2004a. On the cause of the 1930s dust bowl. *Science* **303**: 1855–1859.

Schubert SD, Suarez MJ, Pegion PJ, Koster RD, Bacmeister JT. 2004b. Causes of Long-Term Drought in the United States Great Plains. *Journal of Climate* **17**: 485–503. DOI: 10.1175/1520-0442(2004)017<0485:COLDIT>2.0.CO;2.

Senthil-Kumar AR, Sudheer KP, Jain SK, Agarwal PK. 2005. Precipitation-runoff modelling using artificial neural networks: comparison of network types. *Hydrological Processes* **19**: 1277–1291.

Shrestha RR, Theobald S, Nestmann F. 2005. Simulation of flood flow in a river system using artificial neural networks. *Hydrology and Earth System Sciences* **9**(4): 313–321.

Silva AT, Portela MM, Naghettini M. 2012, Nonstationarities in the occurrence rates of flood events in Portuguese watersheds. *Hydrology and Earth System Sciences Discussions* **8**: 8609–8638. DOI:10.5194/hessd-8-8609-2011.

Smith TM, Reynolds RW, Peterson TC, Lawrimore J. 2007. Improvements to NOAA's historical merged land-ocean surface temperature analysis (1880–2006). *Journal of Climate* **16**: 1601–1612.

Snedecor GW, Cochran WG. 1989. *Statistical methods*, 8th edn, Ames, Iowa State University Press: Iowa, USA.

Sousa PM, Trigo RM, Aizpurua P, Nieto R, Gimeno L, Garcia-Herrera R. 2011. Trends and extremes of drought indices throughout the 20th century in the Mediterranean. *Journal of Natural Hazards Earth System Science* **11**: 33–51.

Trigo RM, Palutikof JP. 2001. Precipitation scenarios over Iberia. A comparison between direct GCM output and different downscaling techniques. *Journal of Climate* **14**: 4422–4446.

Trigo RM, Osborn TJ, Corte-Real JM. 2002. The North Atlantic Oscillation influence on Europe, Climate impacts and associated physical mechanisms. *Climate Research* **20**: 9–17.

Trigo RM, Pozo-Vázquez D, Osborn TJ, Castro-Díez Y, Gámiz-Fortis S, Esteban-Parra MJ, Parra MJ. 2004. North Atlantic oscillation influence on precipitation, river flow and water resources in the Iberian Peninsula. *International Journal of Climatology* **24**: 925–944. DOI:10.1002/joc.1048.

Trigo R, Xoplaki E, Zorita E, Luterbacher J, Krichak SO, Alpert P, Jacobeit J, Sáenz J, Fernández J, González-Rouco F, Garcia-Herrera R, Rodo X, Brunetti M, Nanni T, Maugeri M, Trkes M, Gimeno L, Ribera P, Brunet M, Trigo IF, Crepon M, Mariotti A. 2006. Relations between Variability in the Mediterranean region and mid-latitude variability. In *Mediterranean Climate Variability*, Lionello P, Malanotte-Rizzoli P, Boscolo R (eds). Elsevier: Amsterdam; 179–226.

Vicente-Serrano SM. 2006. Spatial and temporal analysis of droughts in the Iberian Peninsula. *Hydrological Sciences Journal* **51**(1): 83–97.

Vicente-Serrano SM, López-Moreno JI, Lorenzo-Lacruz J, El Kenawy A, Azorin-Molina C, Morán-Tejeda E, Pasho E, Zabalza J, Beguería S, Angulo-Martínez M. 2011. The NAO impact on droughts in the Mediterranean region. In *Hydrological, socioeconomic and ecological impacts of the North Atlantic Oscillation in the Mediterranean region*. Advances in Global Research (AGLO) series, Vicente-Serrano SM, Trigo R (eds). Springer-Verlag: Spain.

Vinther BM, Andersen KK, Hansen AW, Schmith T, Jones PD. 2003. Improving the Gibraltar/Reykjavik NAO Index. *Geophysical Research Letters* **30**(23): 2222. DOI:10.1029/2003GL018220.

Wilhite DA. 2005. *Drought and water crises*. Science, Technology, and Management Issues, CRC Press: Boca Raton, FL, USA.

Wu R, Kinter III JL. 2008. An analysis of the relationship of U.S. droughts with SST and soil moisture: Distinguishing the time scale of droughts. COLA (Center for Ocean-Land-Atmosphere Studies), Technical Report 268.

Xoplaki E, González-Rouco JF, Luterbacher J, Wanner H. 2004. Wet season Mediterranean precipitation variability: influence of large-scale dynamics and predictability. *Climate Dynamiques* **23**: 63–78.

Xue Y, Smith TM, Reynolds RW. 2003. Interdecadal changes of 30-yr SST normals during 1871-2000. *Journal of Climate* **16**: 1601–1612.

Yevjevich V. 1972. *Stochastic Processes in Hydrology*. Water Resour. Publ.: Fort Collins, Co.

Zorita E, Kharin V, VonStorch H. 1992. The atmospheric circulation and sea surface temperature in the North Atlantic area in winter: their interaction and relevance for Iberian precipitation. *Journal of Climate* **5**: 1097–1108.

